10th World Congress on Structural and Multidisciplinary Optimization
May 19 -24, 2013, Orlando, Florida, USA

Multi-Objective Topology Optimization of Multi-Component Continuum Structures via an Explicit Level-Set Approach

Karim Hamza[1], Mohamed Aly[2], Hesham Hegazi[3], Kazuhiro Saitou[4]

[1] University of Michigan, Ann Arbor, USA, khamza@umich.edu
[2] American University in Cairo, Cairo, Egypt, mfawzyaly@aucegypt.edu
[3] Cairo University, Cairo, Egypt, hhegazi@aucegypt.edu
[4] University of Michigan, Ann Arbor, USA, kazu@umich.edu

1. Abstract
This paper explores a framework for topology optimization of multi-component sheet metal structures, such those used in the automotive industry. The primal reason for having multiple components in a structure is to reduce the manufacturing cost, which can otherwise be prohibitively expensive. However, a multi-components structure necessitates re-joining, which comes at sacrifices in assembly cost, weight and structural performance. The problem of designing a multi-component structure is thus posed as in a multi-objective framework. Approaches to solve the problem may be classified into single and two stage approaches. Two-stage approaches focus solely on structural performance at first in order to obtain optimal monolithic (single piece) designs, with the second stage considering decomposition to multiple components and optimizing for all objectives without changing the base topology, which remains identical to that of the monolithic design. Single-stage approaches on the other hand, optimize both base topology and its decomposition simultaneously. Decomposition is an inherently discrete problem, and as such, non-gradient methods are needed for single-stage and second stage of two-stage approaches. This paper adopts an implicit formulation (level-sets) of the design variables, which significantly reduces the number of design variables needed in either single or two stage approaches. The formulation also makes the number of design variables independent from the meshing size, thereby enabling effective application of non-gradient methods to more realistic designs. Test results of a short cantilever study show success of the formulation in both single and two stage approaches, with each approach having different merit.
2. Keywords: Topology Optimization, Multi-Component Structures, Level Sets, Genetic Algorithm

3. Introduction
Topology optimization of continuum structures aims at efficient allocation of structural material within a design domain to perform one or more desirable functions. Much work has been done since the pioneering work of Bendsøe and Kikuchi [1] in terms of applications and methods. Example review articles may be found in [2-4]. Objectives in topology optimization have included compliance minimization and maximization [5-7], stress [8], Eigen frequency [9, 10], crashworthiness [11, 12] and reliability [13]. In most work however, it is either assumed that the structure can be monolithic (manufactured as one piece), or that decomposition into multiple components is an independent problem from the topology optimization. However, decomposition into multiple components is often necessary and/or desirable in large structures due to manufacturability considerations. Common assumptions of prior knowledge about joint locations [14-16] or independence of the decomposition problem from base topology are debatable issues. A very simple example (discussed in detail in [17]) of an in-plane loaded sheet metal structure with a coarse-mesh that allows full enumeration of all possible topologies is shown in Fig. 1. Out of more than two million topologies, about twenty thousand represent feasible multi-component designs, and out of which, 37 are Pareto-optimal in terms of compliance, weight, assembly and manufacturing costs. Notable observations in the example are:

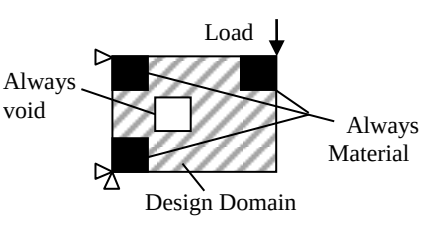

(a) Domain, Loading & Boundary Conditions

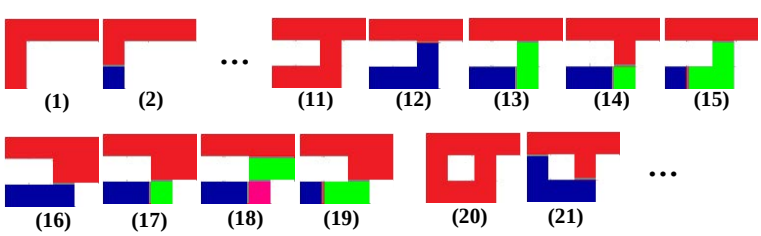

(b) Excerpt Pareto-Optimal Designs

Figure 1: Example simple structure and Pareto-optimal multi-component topologies

i) Monolithic designs (such as solutions 1, 11, 20) are *often* Pareto-optimal for base topologies that have Pareto-optimal solutions. This is likely due to monolithic designs having zero assembly cost, and *usually* less weight and compliance (joints involve sheet folding, and are often less stiff than the base sheet metal)
ii) Monolithic designs are *not always* among the Pareto-optimal solutions however. For example, solutions 16-19 are Pareto-optimal solutions, but the monolithic design with the same base topology is not Pareto-optimal. This is because the monolithic design in question is dominated by solution 20. However, decompositions of that base topology into solutions 16-19 gives different merit compared to solution 20 and its decompositions.

The assumption of independence between the optimization problems of base topology and its decomposition can significantly simplify the design task by adopting two-stage approaches. In two-stage approaches, the base topology is optimized first (via any of the established approaches) as a monolithic structure, and decomposition is considered in a second stage in order to explore options that have better manufacturability [18]. However, two-stage approaches cannot generate all multi-component Pareto-optimal designs, as the ones whose base topology is sub-optimal (such as designs 16-19 in Fig. 1) are not explored. More intuitively, if a design modification to the base topology results in (even small) compromise in structural performance but brings significant improvement in manufacturability, that modification is not explored in two-stage approaches. On the other hand, while adopting a single-stage optimization approach (simultaneously optimizing both the base topology and its decomposition) may eliminate this limitation [18-20], the single-stage optimization may be ineffective in non-gradient problems with a large number of design variables.

Research in topology optimization may be classified from point of view of design variables into explicit and implicit representation. In explicit representation, one design variable is associated with each element in the finite element (FE) mesh, while implicit representations rely on indirect design realization via some domain classifier. Optimization methods that are used may be classified into gradient and non-gradient. Gradient methods [1, 5-10] rely on computing/estimating the sensitivity of objective(s) to changes in the design variables from the results of FE solution, then adjusting the design variables in small increments towards perceived improvements. The main advantage of gradient methods is the capability to handle a very large number of design variables. However, some of the downsides to gradient optimization are possible entrapment in local optima if the objective is non-convex, and the incapability to solve problems that have objectives with no known a gradients. Non-gradient methods such as genetic algorithms (GA) [21, 22] on the other hand can solve for any defined objective(s) and are not easily trapped in local optima. The downsides of non-gradient methods include some inaccuracy and randomness in the obtained solutions (several runs may are often needed to obtain reliable results, which can require a lot more computational resources than gradient methods), and the inefficiency/incapability to solve problems with a large number of design variables. Hybrid methods such as evolutionary structural optimization [23] combine traits of both gradient and non-gradient methods to avoid downsides such as local optima, but also end up inheriting some of the limitations of types of methods such as the reliance on analytical gradients and limitation (though not as sever) on the number of design variables than can be efficiently/reliably solved.

Non-gradient methods using explicit representation received serious critique in [24] with regards to applicability in continuum structures. The main issue is that continuum structures often require hundreds of elements in the FE mesh. Since the number of design variables is equal to the number of elements, non-gradient methods run into serious difficulty even in simple problems. However, with the manufacturing and assembly objectives of interest in this paper not having known gradients, non-gradient methods are inevitable. While previous studies adopting explicit representation [18-20] achieved some success with a relatively coarse (20×10) FE mesh, the limitation of non-gradient optimization is all but too clear even when adopting two-stage approaches.

In order to overcome difficulties in non-gradient optimization, this paper adopts an implicit representation based on level-sets. The level set method is a classification technique [25] that was adopted in topology optimization in the early 2000's [26, 27], in which a scalar level-set function is used to classify the design domain into "structural material" and "void" based on the value of the function relative to some threshold (illustration shown in Fig. 2). Typical level set approaches [26-31] involve a Hamilton-Jacobi system of partial differential equations, with a large number of degrees of freedom, which in turn requires a gradient-based solver. The approach adopted in this paper however, relies on an *explicit level set* (ELS) [32]. Not to be confused with explicit design representations, the adopted formulation is implicit, but based on the ELS definition of the level set function. The word "explicit" in ELS refers to how the function is defined, which is via explicit values at knot points that are interpolated in the rest of the design domain via a Kriging model [33]. The ELS formulation can significantly reduce the number of the design variables and makes it independent from the meshing of the FE model. The reduction in the number of design variables is perceived to significantly improve the effectiveness of non-gradient optimization, and is tested in this paper in both single and two-stage approaches, along with a finer FE mesh than in [18-20].

The paper started with a brief discussion of relevant work and the difficulties associated with the problem of interest. Section 4 provides the details of the mathematical model of the objectives and design variables. Section 5 presents details of the adopted algorithms. Sections 6 conducts several test runs and comparative analysis of a case study of a short cantilever structure. The paper then concludes with a summary and discussion of future work.

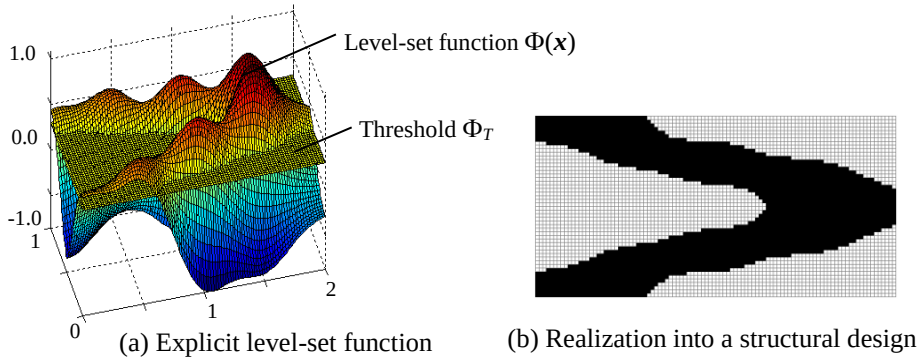

Figure 2: Example explicit level set function in a design domain and its realization into a structural design

4. Problem Formulation

4.1. Generation of Multi-Component Finite Element Models

Evaluating the structural objectives during optimization requires the generation of a multi-component FE model. The FE modeling follows the meshing scheme in [18-20], where a continuum domain (Fig. 3.a) is discretized into ($nElx \times nEly$) large square elements which are termed "main cells" (Fig. 3.b), and represent candidate locations for "structural material". Narrow vertical and horizontal rectangular strip elements, and small square diagonal elements represent candidate locations for joints (Fig. 3.b). The discretized domain corresponds to a ground topology graph (Fig. 3.c), where main cells are represented by the nodes of the graph, while vertical and horizontal elements are represented respectively by horizontal and vertical edges of the graph. Any instance of the design variables (discussed in detail in section 4.2) can be used to generate a product topology graph (Fig. 3.d), which is a sub-graph of the ground topology graph (Fig. 3.c). Graph search techniques are then used to assess the validity of the design, and if valid, a multi-component FE model (Fig. 3.e) that corresponds to the product topology graph is generated, which can then be analyzed via FE analysis in order to evaluate structural performance objectives

In the current formulation, elements in the FE model are assigned "structural material", "joint material" or "void material" (which has very low, but non-zero stiffness in order to avoid numerical singularities in the FE solver). Assigning element material depends on an integer matrix $\tilde{X}$ that is obtained from the graph search. $\tilde{X}$ has dimensions $nElx \times nEly$ and includes the IDs of structural components, with zero indicating void. The procedure for assigning element is as follows:

i) Main cell elements that correspond to a component are assigned structural material, otherwise void material.
ii) Vertical and horizontal elements that have a neighboring void main cell are assigned void material, otherwise they are assigned joint material if they lie between different components, or structural material if enveloped within the same component.
iii) Diagonal elements are assigned void, joint or structural material following the same logic as rectangular elements, but the neighboring checks are conducted verses the rectangular elements it lies in between.

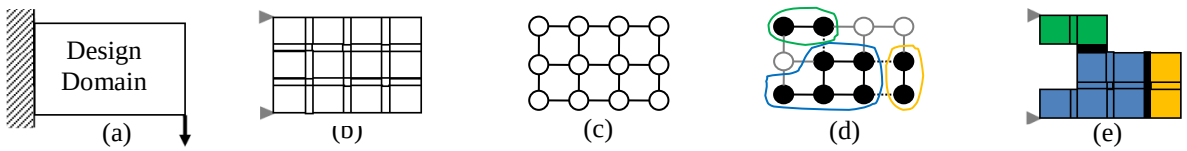

Figure 3: FE modeling outline: (a) Continuum design domain, (b) Discretized design domain, (c) Ground topology graph, (d) a product topology graph, (e) a multi-component structure

Generation of the matrix $\tilde{X}$ from the product topology graph (Fig. 3.d) is done via graph search techniques. The product topology graph is defined via three integer matrices $\boldsymbol{X}$, $\boldsymbol{Y}$, $\boldsymbol{Z}$, which in turn are obtained from the ELS formulation (discussed in detail in section 4.2). Values in the matrices $\boldsymbol{X}$, $\boldsymbol{Y}$, $\boldsymbol{Z}$ are summarized as follows:

$\boldsymbol{X} = \{X_{ij}\}$, $i = 1$ to $nElx$, $j = 1$ to $nEly$, with $X_{ij} = 1$ implying the node (i, j) is part of the product topology graph. $\boldsymbol{X}$, which controls the structural material distribution in the main cell elements, represents the base topology of the structural design

$\boldsymbol{Y} = \{Y_{ij}\}$, $i = 1$ to $nElx - 1$, $j = 1$ to $nEly$, with $Y_{ij} = 1$ implying the horizontal edge between the nodes (i, j), $(i+1, j)$ of the product topology graph is a structural joint

$\boldsymbol{Z} = \{Z_{ij}\}$, $i = 1$ to $nElx$, $j = 1$ to $nEly - 1$, with $Z_{ij} = 1$ implying the vertical edge between the nodes (i, j), $(i, j+1)$ of the product topology graph is a structural joint

Given $\boldsymbol{X}$, $\boldsymbol{Y}$, $\boldsymbol{Z}$, graph search techniques are applied in order to:

i) Check if structural material in main cells is "connected". Example of a disconnected product topology graph (and corresponding structure) is shown in Fig. 4.

ii) If structure is disconnected, calculate a connectivity penalty function P_{con} and set $\tilde{\boldsymbol{X}} = \boldsymbol{0}$

iii) If structure is connected, form the matrix $\tilde{\boldsymbol{X}}$

All the performed graph search tasks rely on well-established one-to-all shortest path algorithms [34]. The connectivity check is done by making a copy of the product topology graph corresponding to $\boldsymbol{X}$, $\boldsymbol{Y}$, $\boldsymbol{Z}$, setting all edges of the temporary graph as "connected" (*i.e.* $\boldsymbol{Y} = \boldsymbol{0}$, $\boldsymbol{Z} = \boldsymbol{0}$), then performing the one-to-all shortest path search from the first node in the graph in an attempt to reach all the other nodes. If some nodes remain unreachable, this implies an invalid disconnected structure.

Forming the matrix $\tilde{\boldsymbol{X}}$ starts by initializing it to zero, then conducting the same procedure of the connectivity check on the temporary graph, but with the graph edges marked as joints in $\boldsymbol{Y}$, $\boldsymbol{Z}$ removed. All the reachable nodes from the first node in the graph are marked as the "first component" in $\tilde{\boldsymbol{X}}$, then the reachable nodes are removed from the temporary graph. The process is repeated for the remaining nodes in the temporary graph, with the reachable nodes marked in $\tilde{\boldsymbol{X}}$ as the "next component", until no more nodes remain in the temporary graph. A connectivity penalty function for disconnected structures is formulated as:

$$P_{con} = P_{con1}(nIslands - 1) + P_{con2}\sum IslandDist \tag{1}$$

Evaluation of the connectivity penalty function follows a similar procedure to forming the matrix $\tilde{\boldsymbol{X}}$, but only to calculate the number of disjoint material "islands" (*nIslands*) and the number of main cells in the shortest paths between them (*IslandDist*). The overall penalty function adds two penalty terms, one term increases with the number of disjointed island segments, and a second term that increases the further apart the disjointed segments are. The weighing of the penalty terms adopted in this paper is by setting $P_{con1} = 100$, and $P_{con2} = 2\,P_{con1} / nElx$. It is noted that the connectivity penalty function only comes to play in single-stage approaches where the base topology $\boldsymbol{X}$ is simultaneously optimized alongside the joint topology. FE analysis is not conducted for disjoint designs, but the penalty function provides the optimization a way of preferring a disjoint design over another based on how close the disjoint designs are to being connected.

Figure 4: Illustration of valid and invalid connectivity in product topology graph and structural designs

4.2. Design Variables

In level sets, a domain classification is performed based on the value of a level set function relative to a threshold (illustration in Fig. 2). For multi-component structures, there are two domain classifications needed; classification into structural material or void, and classification of the structural material into multiple components. As such two level set functions are adopted, with a separate subset of the design variables controlling each function. In the ELS formulation [32], the design variables are simply the explicit values of the level set function at knot points within the design domain, with Kriging models interpolating the value of the functions fitting the knot points, as follows:

$$\Phi_B(\boldsymbol{x}) = w_{Bo} + \sum_{i=1}^{N_B} w_{Bi}\phi_i(\boldsymbol{x}) \tag{2}$$

$$\Phi_J(\boldsymbol{x}) = w_{Jo} + \sum_{i=1}^{N_J} w_{Ji}\phi_i(\boldsymbol{x}) \tag{3}$$

Where $\boldsymbol{x}$ is the spatial position within the design domain. Φ_B, Φ_J are respectively the Kriging interpolations of the base topology and joint topology level set functions. w_{Bi} for $i = 1$ to N_B, and w_{Ji} for $i = 1$ to N_J are the weights of the Kriging models, with N_B and N_J being the number of knot points used for the base topology and joint topology level set functions respectively. A Gaussian covariance function $\phi_i(\boldsymbol{x})$ is calculated for each knot point as:

$$\phi_i(\boldsymbol{x}) = e^{-c^2\|\boldsymbol{x}-\boldsymbol{V}_i\|^2} \tag{4}$$

Where $\boldsymbol{V}_i$ is the spatial position of knot point i, $\|.\|$ is the Euclidean distance and c is a tunable constant that controls the degree overlap between the fitting of knot points, and by extent, the smoothness of level set functions. A parametric study on the tuning of the constant c for single-objective monolithic structures in [32] suggested that the obtainable results via ELS are fairly indifferent to setting of a dimensionless parameter $\tilde{c}$ within the range of 0.35 and 0.7, with the value of c computed according to the formula:

$$c = \frac{1}{\tilde{r}}\sqrt{\ln(1/\tilde{c})} \tag{5}$$

Where $\tilde{r}$ is the minimum Euclidean distance between two knot points. Since the knot points used in the base topology level set function may be different than the ones used for joint topology, it follows that two different values for the constant c are computed for the Gaussian covariance functions in Eqns. 2, 3.
Calculation of the Kriging model weights is done by solving the linear system(s) of equations:

$$\begin{bmatrix} \mathbf{C}_B & \mathbf{1} \\ \mathbf{1}^{\mathrm{T}} & 0 \end{bmatrix} \begin{Bmatrix} \boldsymbol{w}_B \\ w_{Bo} \end{Bmatrix} = \begin{Bmatrix} \boldsymbol{y}_B \\ 1 \end{Bmatrix} \tag{6}$$

$$\begin{bmatrix} \mathbf{C}_J & \mathbf{1} \\ \mathbf{1}^{\mathrm{T}} & 0 \end{bmatrix} \begin{Bmatrix} \boldsymbol{w}_J \\ w_{Jo} \end{Bmatrix} = \begin{Bmatrix} \boldsymbol{y}_J \\ 1 \end{Bmatrix} \tag{7}$$

Where $\boldsymbol{y} = \{\boldsymbol{y}_B{}^{\mathrm{T}}, \boldsymbol{y}_J{}^{\mathrm{T}}\}^{\mathrm{T}}$ is the vector of design variables of the optimization, $\boldsymbol{y}_B = \{y_{Bi}\}^{\mathrm{T}}$ for $i = 1$ to N_B and $\boldsymbol{y}_J = \{y_{Ji}\}^{\mathrm{T}}$ for $i = 1$ to N_J are the values of the level set function at the base topology and joint topology knot points respectively. The matrices $\mathbf{C}_B$ and $\mathbf{C}_J$ are matrices of cross-covariance values between knot points, *i.e.* $\mathbf{C} = \{\mathrm{C_{ij}}\}$, with $\mathrm{C_{ij}} = \phi_i(\boldsymbol{V}_j)$. All design variables in the adopted formulation have the ranges $-1 \le y_i \le 1$, $i = 1$ to $N_B + N_J$.
Classification threshold for the base topology level set function Φ_T is calculated via a line search procedure [32]. For an instance of the design variables $\boldsymbol{y}_B$ dictating the profile of $\Phi_B(\boldsymbol{x})$, increasing the threshold Φ_T means fewer main cell elements will contain structural material, and decreasing it will increase the number of main cell elements containing structural material. Thus, for any instance of the design variables, Φ_T can be adjusted to obtain a desired structural material fraction volume ~~V~~ in the main cells. The classification threshold for the joint topology level set function is simply set to zero, which implies that regions of the design domain that have different sign for Φ_J will belong to different components, with $\Phi_J \approx 0$ being the separation lines. Formation of the matrices $\boldsymbol{X}$, $\boldsymbol{Y}$, $\boldsymbol{Z}$ from the level set functions is done as:

$$X_{ij} = (\overline{X}_{ij} + \widehat{X}_{ij} - \overline{X}_{ij}\widehat{X}_{ij})\breve{X}_{ij} \tag{8}$$

$$\overline{X}_{ij} = \begin{cases} 1 & \text{if } \Phi_B\left(\boldsymbol{x}^1\right) \ge \Phi_T \\ 0 & \text{otherwise} \end{cases} \tag{9}$$

$$Y_{ij} = \begin{cases} 1 & \text{if } \Phi_J\left((\boldsymbol{x}^1\right) \cdot \Phi_J\left(\boldsymbol{x}^2\right) < 0 \\ 0 & \text{otherwise} \end{cases} \tag{10}$$

$$Z_{ij} = \begin{cases} 1 & \text{if } \Phi_J\left(\boldsymbol{x}^1\right) \cdot \Phi_J\left(\boldsymbol{x}^3\right) < 0 \\ 0 & \text{otherwise} \end{cases} \tag{11}$$

$$\boldsymbol{x}^1 = \begin{Bmatrix} (i-1)a+b \\ (j-1)a+b \end{Bmatrix}, \boldsymbol{x}^2 = \begin{Bmatrix} ia+b \\ (j-1)a+b \end{Bmatrix}, \boldsymbol{x}^3 = \begin{Bmatrix} (i-1)a+b \\ ja+b \end{Bmatrix} \tag{12}$$

Where a is the unit cell distance between the centers of main cell elements in the discretized domain, b is half the length of one main cell element, $\widehat{X}_{ij}$ and $\breve{X}_{ij}$ are binary masking matrices for structural material and void. $\widehat{X}_{ij} = 1$ forces the main cell to include structural material, while $\breve{X}_{ij} = 0$ forces the main cell to be void.
When considering single-stage approaches, the number of design variables is equal to $N_B + N_J$, and given an instance of the design variables $\boldsymbol{y}$, Eqns. 2-12 are used for forming the matrices $\boldsymbol{X}$, $\boldsymbol{Y}$, $\boldsymbol{Z}$, which are then analyzed via graph search (as discussed in section 4.1) and employed to generate a multi-component FE model in order to estimate the values of objectives, as discussed in section 4.3. When considering two-stage approaches, the matrix $\boldsymbol{X}$ is first determined via some other topology optimization approach while only considering structural objectives and monolithic structures. In the second stage of two stage approaches, the matrix $\boldsymbol{X}$ is constant and the number of design variable is equal to N_J. Only Eqns. 3-5, 7, 10-12 are needed in order to form the matrices $\boldsymbol{Y}$, $\boldsymbol{Z}$.

4.3. Optimization Problem

The multi-component topology optimization is posed as multi-objective problem as:

$$\text{Minimize } \boldsymbol{f}(\boldsymbol{y}) \tag{13}$$

$$\text{Subject to } \boldsymbol{g}(\boldsymbol{y}) \leq \boldsymbol{0} \tag{14}$$

Where $\boldsymbol{g}(\boldsymbol{y})$ is a vector of constraints, which may contain several constrains on structural performance as a designer sees fit. $\boldsymbol{g}(\boldsymbol{y})$ however contains at least one constraint for the structural connectivity:

$$g_1(\boldsymbol{y}) = P_{con}(\boldsymbol{y}) \leq 0 \tag{15}$$

$\boldsymbol{f}(\boldsymbol{y})$ is a vector of objectives, which may contain one or more structural performance objectives $\{f_1(\boldsymbol{y}), \ldots, f_{nStrObj}(\boldsymbol{y})\}$ pertaining to one or more load cases and/or types of FE analysis. These objectives are calculated from the results of FE analysis. Other than structural performance objectives, the following are considered:
$f_{nStrObj+1}$ is the structural weight, calculated from the FE model
$f_{nStrObj+2}$ is an estimate of assembly cost of all the components in the structure
$f_{nStrObj+3}$ is an estimate of manufacturing cost of all the components in the structure

The assembly cost objective is estimated as a weighed sum of the number of components in a structure (pertains to the number of joining operation and assembly stations) and the total length of welding to be performed. This is summarized as:

$$f_{nStrObj+2}(\boldsymbol{y}) = a_1(nComp - 1) + a_2 L_{welds} \tag{16}$$

The manufacturing cost objective is calculated as the sum of manufacturing cost of all components, which in turn depends on the size and shape complexity of the parts. The model adopted in [19, 20] assumes a polynomial as:

$$f_{nStrObj+3}(\boldsymbol{y}) = \sum_{i=1}^{nComp} \sum_{j,k} m_{jk} A_i^j \psi_i^k \tag{17}$$

Where a_1 and a_2 are assembly cost coefficients associated with the number of joining operation and length of welds respectively. $nComp$ is the number of components in the structure. m_{jk} are the polynomial coefficients for estimating the manufacturing cost, while A_i and ψ_i for i = 1 to $nComp$, are respectively the convex hull area in which a component fits, and the shape complexity factor. The shape complexity factor is calculated based on the model in [35] as the ratio of square of the perimeter to the area:

$$\psi_i = \frac{p_i^2}{A_i} \tag{18}$$

When only considering up to the first order terms in the polynomial, the cost estimate reduces to:

$$f_{nStrObj+3}(\boldsymbol{y}) = \sum_{i=1}^{nComp} \left(m_{00} + m_{01} A_i + m_{10} \psi_i \right) \tag{19}$$

5. Optimization Algorithms

5.1. Overview

Algorithms for optimization of the multi-objective problem formulated in section 4 adopted in this paper rely on NSGA-II [36] along with the crossover and mutation parameters recommended my Michalewiz [37], and a univariate local search [32] which is conducted after the GA runs. In previous studies [18-20], it was observed that the number of quasi-Pareto solutions to the optimization problem in Eqns. 13, 14 can be very large, which can pose a lot of difficulty for single-stage approaches in producing meaningful results. A main perceived reason for this difficulty is that ultra-lightweight designs that have very poor structural performance and/or designs that have decent structural performance but are overly heavyweight (with "dangling" masses) are both easy to generate, and hard to eliminate from the set of undominated solutions in GA, which can clutter the set of undominated solutions and hinders its evolution towards the proper Pareto frontier. To eliminate this difficulty, single-stage approaches in this paper adopt a search intensification strategy, where separate GA runs are conducted for preset/fixed values of $\bar{\boldsymbol{V}} = \{\bar{V}_1, \ldots, \bar{V}_{nVolFrac}\}$ for the material fraction volume of main cell elements. In the second stage of two-stage

approaches, the obtainable solutions are bound to a fixed base topology from the first stage, and values from $\mathbf{V}$ are used (material fraction volume is a required input in most topology optimization approaches) in the first stage to generate the base topology. Summary of the inputs to optimization approaches adopted in this paper are:

1- Domain length, *nElx*, *nEly*
2- Material/void masks: $\hat{X}_{ij}$ and $\breve{X}_{ij}$
3- Material properties of the sheet metal
4- Stiffness and mass properties of joints
5- Loading cases and boundary conditions
6- Cost estimation coefficients for assembly and manufacturing
7- Material fraction volume of main cells to explore $\mathbf{V} = \{V_1, \ldots, V_{nVolFrac}\}$
8- Tuning parameters for the search

Tuning parameters for the search include the number and layout of knot points $\boldsymbol{V}^i$ for i = 1 to $N_B + N_J$, GA population size *nPop* and number of generations *nGen*, number of runs *nSubRuns*, number of Pareto solutions *nSubPareto* to retain for each value of the material fraction volume, as well as the overall number of Pareto solutions *nPareto* to report. A parametric study is conducted in [32] on the choice of knots points, population size and number of generations of the GA for the ELS formulation. Increasing the number of knot points allows more freedom for the level set function, which in turn allows it to properly represent more complex topologies thereby improving the quality of "obtainable" solutions. However, excessively increasing the number of knot points has the downside of increasing the number of design variables, which in turn requires more computational resources for the GA to reliably produce good results. Choices of the tuning parameters in this paper are based off the recommendations in [32] despite that study being based on single objective problems. It may possible to attain better performance by further tuning of the search parameters, but such a task is more difficult in multi-objective problems and is beyond the scope of this paper.

5.2. Single-Stage Approach

Main steps of the adopted algorithm for single-stage optimization are as presented follows:

1. For i = 1 to *nVolFrac* *%% Single Stage: Multi-component structure*
2. $S^i \leftarrow \{\}$
3. For j = 1 to *nSubRuns*
4. Conduct a run of NSGA-II (with a new random number seed) with population size and number of generations *nPop* , *nGen* respectively with consideration of all objectives $\boldsymbol{f}(\boldsymbol{y})$ and constraints $\boldsymbol{g}(\boldsymbol{y})$, and setting V_i as the material fraction volume for calculating the threshold Φ_T
5. Attempt to add all solutions in final population to S^i
6. Limit the number of solutions retained in S^i to only *nSubPareto* solutions
7. Next j
8. Next i
9. $\tilde{S} \leftarrow \{ S^1, \ldots, S^{nVolFrac}\}$
10. Limit the number of solutions retained in $\tilde{S}$ to only *nPareto* solutions
11. $S \leftarrow \{\}$
12. For i = 1 to *nPareto*
13. Run univariate search from starting point solution i in $\tilde{S}$
14. Attempt to add result of the univariate search to S
15. Next i
16. Return S

The univariate search (line 13), adopted from [32] attempts to adjust each design variable at a time. If adjustment of a variables results in improving the solution, the new solution replaces current one and the process is repeated. Reducing the number of solutions in a set of undominated solutions (lines 6, 10) is based on retaining the solutions having largest "crowding distance" [36], which keeps the retained solutions well spread-out on the undominated frontier. The "attempt to add solution" (lines 5, 14) involves two checks:

i) If candidate solution is Pareto-dominated by any solution in the solution set, it is not added
ii) If candidate solution dominates any solution in the solution set, the dominated solutions are removed

5.3. Two-Stage Approach

Main steps of the adopted algorithm for two-stage optimization are as presented follows:

1. For i = 1 to *nVolFrac* *%% First Stage: Base topology monolithic structure*
2. Run topology optimization considering only the structural objectives and monolithic structure to obtain a base topology $\boldsymbol{X}^i$ for material fraction volume $\bar{V}_i$
3. Next i
4. For i = 1 to *nVolFrac* *%% Second Stage: Multi-component structure*
5. $S^i \leftarrow \{\}$
6. For j = 1 to *nSubRuns*
7. Conduct a run of NSGA-II (with a new random number seed) with population size and number of generations *nPop* , *nGen* respectively with consideration of all objectives $\boldsymbol{f}(\boldsymbol{y}_J \mid \boldsymbol{X}^i)$
8. Attempt to add all solutions in final population to S^i
9. Limit the number of solutions retained in S^i to only *nSubPareto* solutions
10. Next j
11. Next i
12. $\tilde{S} \leftarrow \{ S^1, \ldots, S^{nVolFrac}\}$
13. Limit the number of solutions retained in $\tilde{S}$ to only *nPareto* solutions
14. $S \leftarrow \{\}$
15. For i = 1 to *nPareto*
16. Run univariate search from starting point solution i in $\tilde{S}$
17. Attempt to add result of the univariate search to S
18. Next i
19. Return S

6. Case Study

A study of the performance of single and two stage approaches is conducted for a short cantilever structure whose boundary conditions and loading are shown in Fig. 5. Only one loading case is considered and one structural performance objective, with is the minimization of compliance at the loading point. Material properties (assuming mild steel) and cost estimation coefficients are summarized in Table 1. It is noted that the joints model assumes lap joints, hence the 2.0 multiplier on the mass of joint elements due to overlapping sheets and the isoperimetric in-plane stiffness behavior, with somewhat less stiffness than the base sheet metal [38]. Tuning parameters for the optimization algorithms are listed for single and two-stage approaches in Table 2.

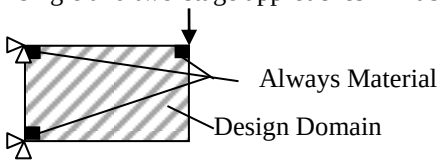

Figure 5: Design domain and boundary conditions for short cantilever problem

Table 1: Material properties and cost estimation coefficients

Parameter	Value	Unit
Young's Modulus	207	GPa
Poisson's Ratio	0.3	
Density	7800	kg/m^3
Design domain length	2.0	m
nElx	40	
nEly	20	
Sheet metal thickness (t)	1.2	mm
Length to width ratio of rectangular elements	10:1	
Joint elements mass multiplier	2.0	
Joint elements stiffness multiplier	0.65	
Assembly cost coefficient (a_1)	1.00	$
Assembly cost coefficient (a_2)	5.00	$/m
Manufacturing cost coefficient (m_{00})	0.00	$
Manufacturing cost coefficient (m_{10})	1.0	$/m^2
Manufacturing cost coefficient (m_{01})	4.0×10^{-4}	$

Table 2: Tuning parameters for optimization algorithms

Parameter	Single-stage	Two-stage
Material fraction volume in main cells	{0.45, 0.5, 0.55, 0.6}	{0.45, 0.5, 0.55, 0.6}
Base topology knot points	41 points, zigzag grid	–
Joint topology knot points	15 points, square grid	15 points, square grid
nPop	150	80
nGen	400	120
nSubRuns	5	5
nSubPareto	30	30
nPareto	50	50

A total of five complete runs were conducted for both single and two stage approaches following the steps discussed in sections 5.2 and 5.3 respectively. Normalized Pareto-plots (objective values scaled with respect to maximum and minimum among the undominated set of solutions) from all runs are shown in Fig. 6, and select structural designs are shown along with spider-web diagrams of the objective values in Fig. 7. The base topology in two-stage approaches was generated via power-law method using publicly available code [6] for the respective values of material fraction volume. Monolithic designs corresponding to the base topology are observed among the undominated set of solutions (designs B1, B4, B7, B10 in Fig. 7). It is observed in Fig. 6 that the Pareto may be including a very large number of solutions, and in earlier tests, single stage approaches had most of the solutions drifting towards low manufacturing cost with poor structural performance regions of the Pareto set. To remedy this, an additional constraint $g_2(\boldsymbol{y})$ was imposed to eliminate those uninteresting regions of the Pareto set. $g_2(\boldsymbol{y})$ required the compliance to be no more than three times the minimum for the respective material fraction volume (from designs B1, B4, B7, B10). Limits of $g_2(\boldsymbol{y})$ are sketched in Fig.6.

Run-1 through Run-5 in Fig. 6 are single-stage runs, while Run-6 through Run-10 are two-stage runs. Fig. 7 is organized in increasing order of material fraction volume and type of approach used: Designs A1-A3 and B1-B3 have the least, while A10-A12 and B10-B12 have the largest material fraction volume respectively. Designs A1-A12 are from single-stage runs, while designs B1 through B12 are from two-stage runs. It is understandably evident that material fraction volume in the main cells is the major controlling factor for the structural weight objective f_2 with decomposition into multiple components having some, but little effect on it. It is also observed that fixing the base topology all but locks the value of the structural compliance objective f_1. With weight and stiffness not changing much via decomposition of a base topology two-stage results appear lumped into narrow spots in the $f_1 - f_2$ plot in Fig. 6. While designs obtained via the two-stage approach appear to dominate those obtained from single-stage approach in $f_1 - f_2$ plot, the opposite appears to be true in $f_3 - f_4$ plot. This implies that single and two stage approaches appear to be converging to different regions of the Pareto frontier. When structural performance is the most important, two-stage approach are recommended since the solutions returned include only minimal compromises from best attainable structural performance. Two-stage approach also involves fewer design variables, which means less requirement for computational resources. Run-time benchmarking on an Intel i5 processor produced approximately 5 and 36 hours to complete one run for two and single stage approaches respectively. When cost is important and some compromise in structural performance is acceptable however, the single-stage approach can be useful since it explores alternative base topologies (two-stage approach does not).

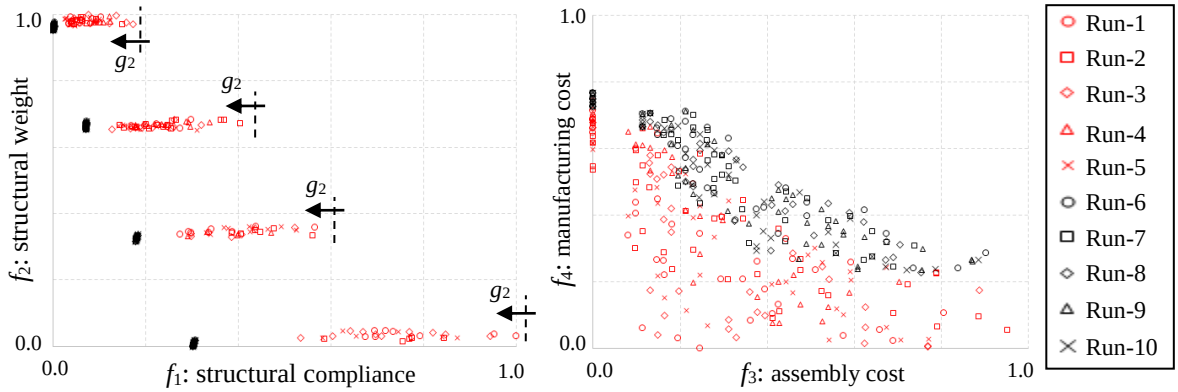

Figure 6: Normalized Pareto-plots for conducted runs of single and two stage approaches

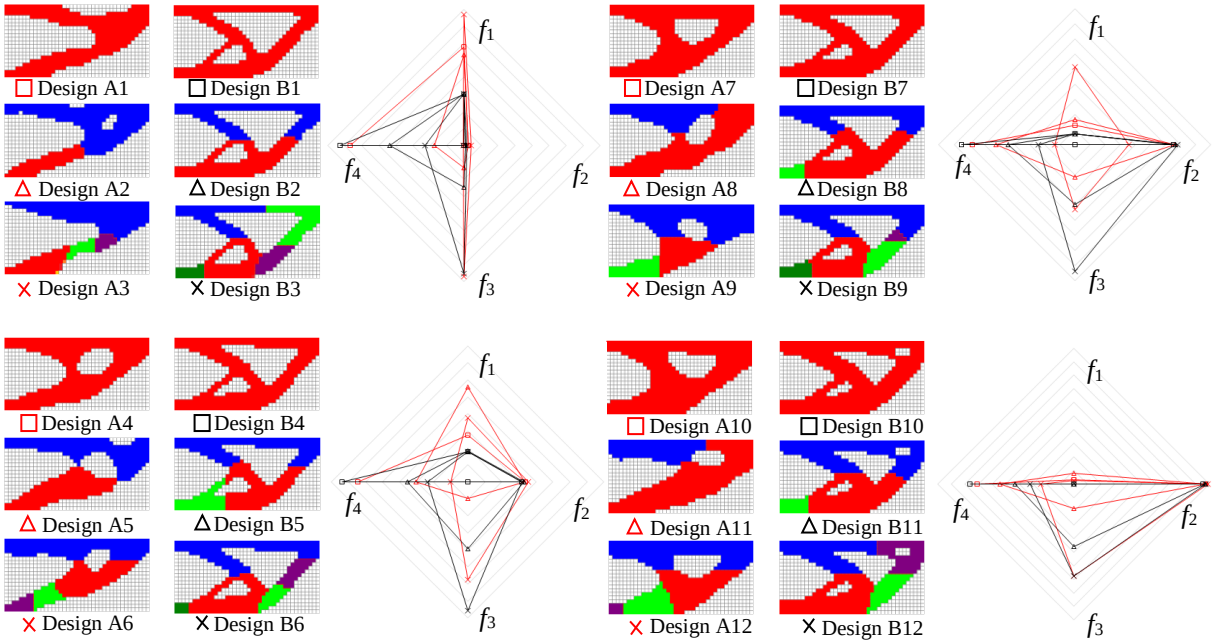

Figure 7: Details of select designs from single and two stage runs undominated solutions

A quantitative comparison is conducted between the solutions obtained from the various runs via the "C-metric" [39], which is a means for comparing sets of solutions for multi-objective problems. Given two sets of solutions S^1 and S^2, the C-metric $\complement_{12}$ is the fraction of solutions in S^1 that are dominated by at least one solution in S^2. Pairwise values of the C-metric are listed in Table 3 for the 10 conducted runs, and global C-metric values (fraction of solutions in a solution set dominated by any solution in any of the other runs) are listed in Table 4. Among the notable observations in Table 3 is that none of the two-stage runs (runs 6-10) contain solutions that are dominated by any of the solutions generated by single-stage runs (runs 1-5), which is understood since f_1 value in all solutions in two-stage runs (Fig. 6) is less its best value in single-stage runs at each material fraction volume. Most (but not all) single-stage runs do include solutions dominated by two-stage runs. However, the percentile appears to about 10% at most. On the other hand, pairwise dominance among runs of the same approach appear to reach much higher percentiles (up to 18-22%). This is indicative that the random variations in GA results are more pronounced than the dominance between single and two stage approaches, which further supports the assessment that single and two stage approaches are generating solutions at different regions of the Pareto frontier. Table 4 shows the global C-metric indicating appreciable percentile of sub-optimal solutions in each run, which may hint that further tuning is needed for (*nPop*, *nGen*, *nSubRuns*), or that multiple runs per problem are recommended.

Table 3: Pairwise C-metric values for conducted single and two stage runs

Run	1	2	3	4	5	6	7	8	9	10
1	-	0.064	0.085	0.043	0.128	0.000	0.000	0.000	0.000	0.000
2	0.087	-	0.087	0.022	0.130	0.000	0.022	0.000	0.022	0.022
3	0.128	0.106	-	0.064	0.170	0.064	0.064	0.064	0.064	**0.106**
4	**0.182**	**0.182**	0.159	-	0.182	0.068	0.091	0.091	0.068	0.091
5	0.021	0.064	0.149	0.021	-	0.000	0.021	0.000	0.000	0.000
6	0.000	0.000	0.000	0.000	0.000	-	0.146	0.104	0.167	0.083
7	0.000	0.000	0.000	0.000	0.000	0.021	-	0.085	0.128	0.043
8	0.000	0.000	0.000	0.000	0.000	0.063	0.125	-	0.146	0.104
9	0.000	0.000	0.000	0.000	0.000	0.060	0.100	0.020	-	0.040
10	0.000	0.000	0.000	0.000	0.000	0.082	**0.224**	0.082	0.163	-

Table 4: Global C-metric values for conducted single and two stage runs

Run	1	2	3	4	5	6	7	8	9	10
Global C-metric	0.298	0.152	0.340	0.432	0.213	0.313	0.191	0.271	0.140	0.245

7. Conclusion and Future Work

This paper adopted ELS formulation to multi-objective topology optimization of multi-component structures. Since assembly and manufacturing objectives having no known analytical gradients, non-gradient optimization approaches such as GA are needed. The ELS formulation makes the number of design variables independent of the meshing size, which is beneficial to both single and two stage optimization approaches, as it enables the use of mesh sizes that appropriately model realistic sheet metal structures. Single and two stage approaches were tested on a cantilever structure, and appeared to have different merits. Two-stage approaches can take advantage of well-established topology optimization methods to produce designs that have the best structural objectives and/or minimal compromise from it. Single stage approach may require additional constraints on minimum acceptable structural performance in order to eliminate uninteresting solutions and require almost an order of magnitude more computational resources than two stage approaches. The advantage of single-stage approach however is that it can search for alternative base topologies and hence better opportune for improvement in manufacturing and assembly costs despite some compromise in structural performance objectives.

While adoption of ELS formulation could be a milestone in multi-component topology optimization, future work may flow in one or more directions: i) more general FE models such as shell elements and mapped regions instead of a rectangular plane domains, ii) multiple thicknesses and material options for the components, iii) multiple joint types, iv) more refined models for assembly and manufacturing such as inclusion of higher order polynomial terms, and v) algorithmic refinements such as GA population seeding and further tuning of the search parameters.

8. References

1. M.P. Bendsøe and N. Kikuchi, Generating optimal topologies in structural design using a homogenization method, *Computer Methods in Applied Mechanics and Engineering*, 71, 197-224, 1988.
2. G. Rozvany, Aims, scope, methods, history and unified terminology of computer-aided topology optimization in structural mechanics, *Structural and Multidisciplinary Optimization*, 21(2), 90-108, 2001.
3. K. Saitou, S. Nishiwaki, K. Izui, P. Papalambros, A survey on structural optimization in product development, *Journal of Computing and Information Science in Engineering*, 5(3), 214-226, 2005.
4. G. Rozvany, A critical review of established methods of structural topology optimization, *Structural and Multidisciplinary Optimization*, 37, 217-237, 2009.
5. M.P. Bendsøe, Optimal shape design as a material distribution problem, *Structural Optimization*, 1, 193-202, 1989.
6. O. Sigmund, A 99 line topology optimization code written in MATLAB, *Structural and Multidisciplinary Optimization*, 21(2), 120-127, 2001.
7. X. Liu, E. Lee, H.C. Gea, P.A. Du, Compliant mechanism design using a strain based topology optimization method, *ASME IDETC*, DETC2011-48525, Washington DC, 2011.
8. G. Allaire, F. Jouv, H. Maillot, Topology optimization for minimum stress design with the homogenization method, *Structural and Multidisciplinary Optimization*, 28. 87-98, 2004.
9. A. Diaz, N. Kikuchi, Solutions to shape and topology eigenvalue optimization using a homogenization method, *International Journal for Numerical Methods in Engineering*, 35, 487-502, 1992
10. Z-D. Ma, N. Kikuchi, H-C. Cheng, Topological design for vibrating structures, *Computer Methods in Applied Mechanics and Engineering*, 121(1-4), 259-280, 1995
11. R. Mayer, N. Kikuchi, R. Scott, Application of topological optimization techniques to structural crashworthiness, *International Journal for Numerical Methods in Engineering*, 39(8), 1383-1403, 1996.
12. H.C. Gea, J. Luo, Design for energy absorption: a topology optimization approach, *ASME IDETC*, DAC-21060, Montreal, QC, 2001.
13. G. Kharmanda, N. Olhoff, A. Mohamed, M. Lemaire, Reliability-based topology optimization, *Structural and Multidisciplinary Optimization*, 26(5), 295-307, 2004.
14. T. Jiang and M. Chirehdast, A Systems Approach to Structural Topology Optimization: Designing Optimal Connections, *Journal of Mechanical Design*, 119, 40–47, 1997.
15. H. Chickermane, H.C. Gea, Design of Multi-Component Structural System for Optimal Layout Topology and Joint Locations, *Engineering Computations*, 13, 235–243, 1997.
16. Q. Li, G.P. Steven, Y.M. Xie, Evolutionary structural optimization for connection topology design of multi-component systems, *Engineering Computations*, 18(3-4), 460-479, 2001.
17. Z. Zhou, K. Hamza, K. Saitou, Decomposition Templates and Joint Morphing Operators for Genetic Algorithm Optimization of Multi-Component Structural Topology, *Journal of Mechanical Design*, in review.
18. A. Yildiz, K. Saitou, Topology Synthesis of Multi-Component Structural Assemblies in Continuum Domains, *Journal of Mechanical Design*, 133, 011008, 2011.
19. Z. Zhou, K. Hamza, K. Saitou, Multi-Objective Topology Optimization of Spot-Welded Planar Multi-Component Continuum Structures, *9th World Congress on Structural and Multidisciplinary Optimization*, Shizuoka, Japan, 2011.

20. Z. Zhou, K. Hamza, K. Saitou, Decomposition Templates and Joint Morphing Operators for Genetic Algorithm Optimization of Multi-Component Structural Topology, *ASME IDETC*, DETC2011-48572, Washington DC, 2011.
21. K. Deb, S. Gulati, Design of Truss-Structures for Minimum Weight Using Genetic Algorithms, *Finite Elements in Analysis and Design*, 37(5), 447-465, 2001.
22. A. Madeira, J.F. Rodrigues, H. Pina, Multi-Objective optimization of structures topology by genetic algorithms, *Advances in Engineering Software*, 36, 21-28, 2005.
23. Y.M. Xie, G.P. Steven, A simple evolutionary procedure for structural optimization, *Computers and Structures*, 49(5), 885-896, 1993.
24. O. Sigmund, On the usefulness of non-gradient approaches in topology optimization, *Structural and Multidisciplinary Optimization*, 43, 589-596, 2011.
25. S. Osher, J.A. Sethian, Front propagating with curvature dependent speed: algorithms based on Hamilton–Jacobi formulations, *Journal of Computational Physics*, 78, 12-49, 1988.
26. G. Allaire, F. Jouve, A.M. Toader, Structural optimization using a sensitivity analysis and a level-set method, *Journal of Computational Physics*, 194, 363-393, 2004.
27. M.Y. Wang, X. Wang, D. Guo, A level set method for structural topology optimization, *Computer Methods in Applied Mechanics and Engineering*, 192, 227-246, 2003.
28. S. Wang, M.Y. Wang, Radial basis functions and level set method for structural topology optimization, *International Journal for Numerical Methods in Engineering*, 65, 2060–2090, 2006.
29. P. Wei, M.Y. Wang, Piecewise constant level set method for structural topology optimization, *International Journal for Numerical Methods in Engineering*, 78, 379-402, 2009.
30. T. Yamada, K. Izui, S. Nishiwaki, A. Takezawa, A topology optimization method based on the level set method incorporating a fictitious interface energy, *Computer Methods in Applied Mechanics and Engineering*, 199, 2876-2891, 2010.
31. James, K. A., Martins, J. R. (2012). "An isoparametric approach to level set topology optimization using a body-fitted finite-element mesh," Computers and Structures, 90-91: 97-106
32. K. Hamza, M. Aly, H. Hegazi, An Explicit Level-Set Approach for Structural Topology Optimization, *ASME IDETC*, DETC2013-12155, Portland, OR, 2013.
33. T. Simpson, A. Booker, D. Ghosh, A. Giunta, P. Koch, R.J. Yang, Approximation Methods in Multidisciplinary Analysis and Optimization: A Panel Discussion, *Structural and Multidisciplinary Optimization*, 27, 302-313, 2004.
34. E.V. Denardo, *Dynamic Programming: Models and Applications*, Dover Publications, Mineola, NY, 2003.
35. G. Boothroyd, P. Dewhurst, W. Knight, *Product Design for Manufacturing and Assembly*, Marcel Dekker, New York, 1994.
36. K. Deb, A. Pratap, S. Agarwal, T. Meyarivan, A fast and elitist multiobjective genetic algorithm: NSGA-II, *IEEE transactions on evolutionary computation*, 6(2), 182-197, 2002.
37. Z. Michalewiz, and D. Fogel, *How to Solve it: Modern Heuristics*, Springer-Verlag Berlin Heidelberg, New York, 2000.
38. S. Xu, X. Deng, An evaluation of simplified finite element models for spot-welded joints, *Finite Element in Analysis and Design*, 40, 1175-1194, 2004.
39. E. Zitler, L. Thiele, Multi-objective evolutionary algorithms: a comparative case study and the strength Pareto approach, *IEEE transactions on evolutionary computation*, 3(4), 257-271, 1999.